

RSC Advances



This is an *Accepted Manuscript*, which has been through the Royal Society of Chemistry peer review process and has been accepted for publication.

Accepted Manuscripts are published online shortly after acceptance, before technical editing, formatting and proof reading. Using this free service, authors can make their results available to the community, in citable form, before we publish the edited article. This *Accepted Manuscript* will be replaced by the edited, formatted and paginated article as soon as this is available.

You can find more information about *Accepted Manuscripts* in the [Information for Authors](#).

Please note that technical editing may introduce minor changes to the text and/or graphics, which may alter content. The journal's standard [Terms & Conditions](#) and the [Ethical guidelines](#) still apply. In no event shall the Royal Society of Chemistry be held responsible for any errors or omissions in this *Accepted Manuscript* or any consequences arising from the use of any information it contains.

Cite this: DOI: 10.1039/c0xx00000x

www.rsc.org/xxxxxx

ARTICLE TYPE

Ionic Liquids Based Vibration Energy Harvester by Periodically Squeezing Liquid Bridge

Weijie Kong,^a Pengfei Cao,^a Xiaodong He,^a Long Yu,^a Xiangyuan Ma,^b Yude He,^b Liujin Lu,^b Xiaoping Zhang*^a and Youquan Deng*^b

⁵ Received (in XXX, XXX) Xth XXXXXXXXXX 20XX, Accepted Xth XXXXXXXXXX 20XX

DOI: 10.1039/b000000x

This paper presents ionic liquids based vibration energy harvester by periodically squeezing liquid bridge, which has excellent characteristics such as no need of airtight space, wide operating temperature range (which is up to 100 °C) and in particular improved output power at high temperatures.

Energy harvesting from the ambient vibration as a potential power sources for autonomous sensors and portable applications with small power consumption are drawing much attentions ¹. Existing methods of mechanical-to-electrical energy conversion are piezoelectric ², electromagnetic ³ and electrostatic ^{4, 5}. Each of them has their respective advantage and disadvantage. In the case of the electrostatic approach, it uses a variable capacitor structure to generate electrical power and the electrostatic devices are easier to integrate in microsystem, low cost and simple structure with less circuitry. Most importantly, the electrostatic devices are very suitable for low-frequency (<100 Hz) and low-amplitude vibration sources. But their output powers are too low to power small electronic devices. Microfluidics ⁶ is a burgeoning multidisciplinary field interesting engineering, physics, chemistry, nanotechnology and biotechnology, with practical applications to the design of systems in which small volumes of fluids (fL to μL) will be handled. Because of the flexibility and miniaturization, microfluidics-based devices are very suitable for effective converting the many high-power mechanical energy sources to electricity in small size which can improve the generated power. In 2011, combined with the microfluidics technology and electrostatic method, a new approach to energy harvesting has been proposed ⁷. The approach runs the electrowetting in reverse and converts the mechanical energy of liquid (Mercury and Galinstan) motion into electrical energy. Supplied by the external DC bias-voltage source, energy generation is achieved by squeezing the microscopic liquid droplets between vibrating plates. And the output power has been largely improved. Unfortunately, it is not very practical for needing of external bias-voltage source and mercury has the toxicity. In order to overcome these disadvantages, Moon et al. present a new method - AC electrical power is generated by mechanically modulating electrical double layers ⁸. When the height of the water bridge is mechanically modulated, the electrical double layer

capacitors (EDLCs) ^{9, 10} formed on the two interfacial areas between bridge and conducting plates are continuously charged and discharged at different phases from each other, which generates the electrical power. However, the liquid media in this approach is the deionized water with trace impurities. Water always evaporates in the air in natural condition and thus the power output decreases with time accordingly. Furthermore, the water based setup can not work at relatively high or low temperatures (such as 100 °C or 0 °C). Therefore, development of liquid media with low volatility and toxicity, wide liquid temperature range and high power output for microfluidics based vibration energy harvester (VEH) should be highly desirable.

Room temperature ionic liquids (RTILs or ILs) have emerged as a novel class of versatile solvent and soft material due to their negligible vapor pressure, wide liquid temperature range, acceptable electrochemistry stability, non-toxicity and environment friendly ¹¹. Besides these well-known properties, the most important characteristic of ILs is that their properties can be significantly regulated for any particular application by changing their ions combination. This makes them “designable materials”. These excellent physicochemical properties render them potential candidates for microfluidics-based VEH.

In this paper, we firstly propose the VEH using ILs, which can overcome the mentioned problems above while keeping high power output. That is, the ILs based VEH can work without airtight space and at high or low temperatures.

Five imidazolium ILs, [EMIm][N(CN)₂], [BMIm][N(CN)₂], [EMIm][BF₄], [EMIm][SCN] and [BMIm][NO₃] were synthesized according to established procedures. The ILs purity > 99%. The viscosity, ion conductivity, surface tension and density of all ILs were also measured (Table S1 in the ESI†). According to the structure of water based VEH prototype ⁸, the ILs based VEH prototype is composed of two parallel conducting plates and ILs bridge between them, as shown in Fig. 1(a). The top plate (ITO glass) was covered with hydrophobic layers (Teflon AF) and the bottom plate is hydrophilic ITO glass. Because the two EDLCs are formed on the contact surfaces between ILs bridge and conducting plates, the electric circuit model can be expressed as shown in Fig. 1(b), which includes two EDLCs C_T and C_B , a electric resistor R_F denoting the ILs bridge resistance and a resistive load R_L .

When the ILs bridge between the plates is periodically squeezed by vertically vibrating the bottom plate, the top contact area changes periodically due to the hydrophobicity of top surface and it results in the variation of top EDLC capacitance, while the bottom contact area does not change obviously due to the small contact angle and pinning effects of the hydrophilic bottom surface and thus bottom EDLC capacitance does not change appreciably. Fig. 1(c-d) show that each periodic change of top EDLC capacitance results in the variation of total charge stored in top EDLC and the part free charge flows from bottom EDLC to top EDLC (when top EDLC increasing) or from top EDLC to bottom EDLC (when top EDLC decreasing) in electric circuit, which generates AC electrical power. The quite different wetting properties of two conducting plates make the top contact area increase for improving output power. The differential equation⁸ based on the electric circuit model shown in Fig. 1(b) is used to numerical calculates (Electric Circuit Model and Numerical Calculations in the ESI†). The voltage drop across the load resistance is measured and the effective power is calculated by root-mean-square (RMS) voltage. Besides, the generated power improves by increasing the volume of IL bridges and the maximum volumes of the IL bridges are determined by the capillary length of ILs, which is $\kappa^{-1} = \sqrt{\gamma / \rho g}$ ⁸. In this expression, γ , ρ and g are the surface tension, density of ILs and gravitational acceleration, respectively. By simply geometric calculation, the maximum volume of the IL bridges is the volume of half sphere with radius of the capillary length. When the volume of droplet exceeds the maximum volume, the ILs droplet degenerates pancake shape¹², which will reduce the power generation substantially. For the ILs discussed in this paper, all their maximum volumes are larger than about 15 μL . Consequently, the volumes of liquid bridges are set to 15 μL for convenience of comparison and high power output.

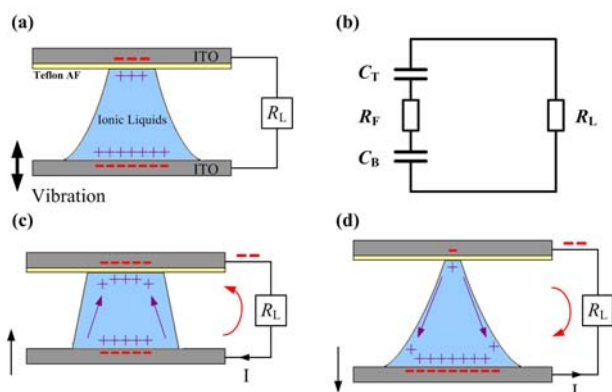


Fig. 1 Schematic diagram of the experiment and the electric circuit model.

Figure 2 demonstrates the calculated and measured instantaneous output voltage and the corresponding instantaneous power across the load resistor when a 15 μL [EMIm][N(CN)₂] bridge is positioned. When vibrating the bottom plate according to $L\sin(2\pi ft)$, the instantaneous output voltage fluctuates with positive and negative peaks, where L , f and t are vibration amplitude, frequency and time, respectively. In terms of the measured data, the maximum

negative voltage and positive voltage are respectively about 389 mV and 182 mV. Correspondingly, the maximum instantaneous power and effective power are about 5.0 nW and 1.2 nW, respectively. The contact areas between liquid bridge and conducting plates are measured for numerical calculation. The maximum and minimum top contact areas at the vibration amplitude of 0.35 mm and frequency of 10 Hz are about 14.8 mm² and 4.8 mm², respectively, and the top contact area variation in calculation is approximated by the sine function of $9.8 + 5.0\sin(20\pi t)$ mm². When decreasing the amplitude, the top contact area variation will decrease. The bottom contact area is about 17.2 mm² and nearly constant in experiments due to small contact angle and pinning effects. It is obvious that that the calculated results based on electrical circuit model good match the measured results, but deviate the detailed waveform near the positive voltage peak. This may be speculated that the experimental contact area between the ILs bridge and top plate is not exact sinusoidal variation because of the hydrodynamic flow in ILs bridge and imperfections in the surface of the Teflon-coated top plate, while the contact area in calculations is.

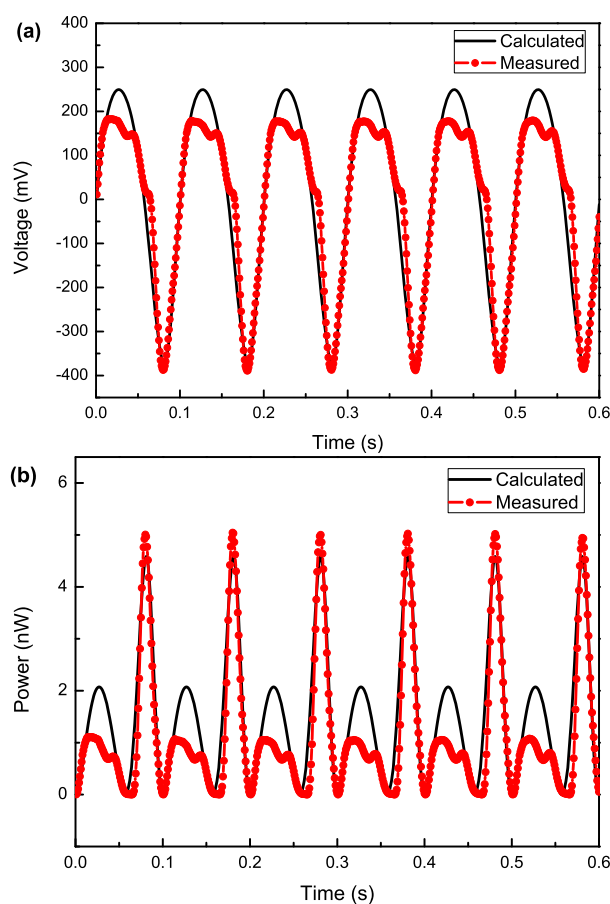


Fig. 2 (a) Instantaneous voltage and (b) instantaneous power generated by a bridge of [EMIm][N(CN)₂] for a sinusoidal vibration with $f=10$ Hz, $L=0.35$ mm and $R_L=30$ M Ω , and corresponding calculated data. Volume of bridge is 15 μL . The liquid-substrate overlap area for a single liquid bridge is about 17.2 mm². The maximum and minimum top contact areas are about 14.8 mm² and 4.8 mm², respectively.

The dependence of the power generation on the vibration amplitude and frequency with different ILs are investigated

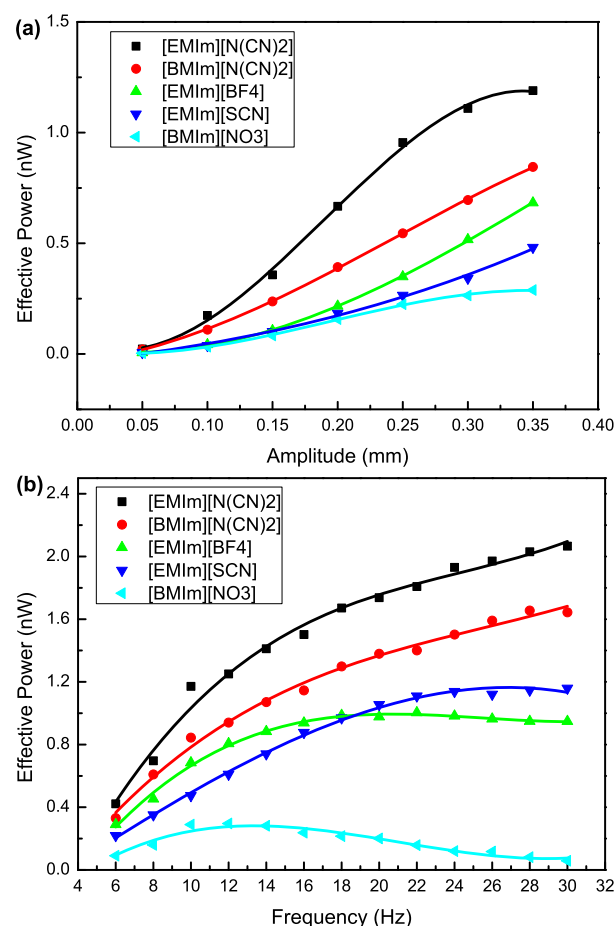


Fig. 3 (a) The effective power versus vibration amplitude L for five typical ILs with $f=10$ Hz and $R_L=30$ M Ω . (b) The effective power versus vibration frequency f for five typical ILs with $L=0.35$ mm and $R_L=30$ M Ω . Volumes of bridges are 15 μ L. Dots represent the actual experimental data while solid lines are the fitted results.

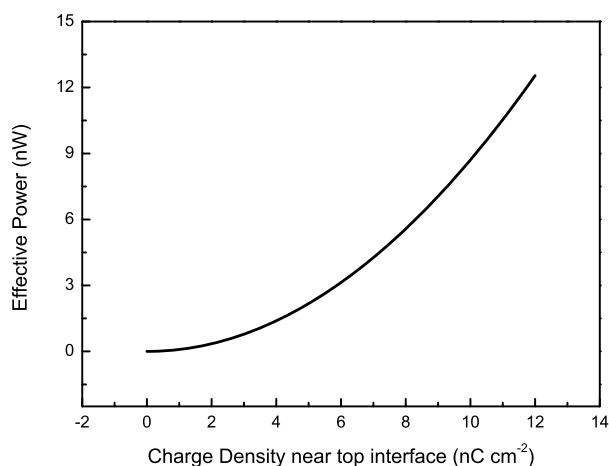


Fig. 4 The effective power versus charge density near top interface of VEH according to the electric circuit model.

for a sinusoidal vibration as shown in Fig. 3. We can see that the effective power increases with vibration amplitude for all five kinds of ILs in a limited range. The variation of the contact area between the ILs bridge and top plate increases with vibration amplitude. Large variation of the contact area leads to increase of the top EDLC capacitance variation and

thus the free charge flowing across load increases, which results in the increase of the power generation. Meanwhile, in the same vibration amplitude of 0.35 mm and frequency of 10 Hz, the output power presents $P_{[EMIm][N(CN)_2]} > P_{[BMIm][N(CN)_2]} > P_{[EMIm][BF_4]} > P_{[EMIm][SCN]} > P_{[BMIm][NO_3]}$. The most important two reasons are the differences of the charge densities near top interfaces between conducting plates and IL bridges, and the differences of the IL viscosities. High charge density near top interface leads to the increase of the charge stored in top EDLC and therefore the free charge flowing through the electrical circuit when the variation of the top EDLC capacitance keeps constant (i. e. the top contact area variation is nearly constant). Thus the output power increases sharply with charge density near top interface. The consistent conclusion is also obtained by the electric circuit model prediction as shown in Fig. 4. Moreover, the viscosity can also influence the output power. Low viscosity guarantees large variation of the contact area between the ILs bridge and top plate during the vibration cycle and therefore the output power increases. The two main factors jointly determine the generated power. Particularly, the structures of ILs primarily influence the charge density near top interface and viscosity, and thus the output power depends on that substantially. For [N(CN)₂]⁻-based ILs with different cations - [EMIm][N(CN)₂] and [BMIm][N(CN)₂], absorption of the cation to top plate becomes stronger as the length of the alkyl chain decreases¹³, which results in the increase of the charge density near the top interface. Further, the viscosity of ILs with longer alkyl chain are larger, as a consequence, $P_{[EMIm][N(CN)_2]} > P_{[BMIm][N(CN)_2]}$. For [EMIm]⁺-based ILs with different anions and nearly same viscosities - [EMIm][N(CN)₂] and [EMIm][SCN], $P_{[EMIm][N(CN)_2]} > P_{[EMIm][SCN]}$, the reasons are maybe the differences of the anion size, cation-anion interaction and the top surface-anion interaction, which cause to existence of the more cations and less anions in the vicinity of top interface for [EMIm][N(CN)₂]. As a result, the larger charge density of [EMIm][N(CN)₂] near top interface generates more power. In this work, the vibration frequency is not more than 30 Hz because the complex hydrodynamic effects at high frequency will deform ILs bridge^{14,15}. From the observation of Fig. 3(b), for ILs with relatively large viscosity - [BMIm][NO₃], [EMIm][BF₄] and [BMIm][N(CN)₂], the effective power increases at first, reaches the maximum and then decreases with vibration frequency. It arises from the negative impact of viscosity induced damping on change of the top contact area outpaces the positive impact of frequency increase when the vibration frequency is relatively high. Moreover, the optimal frequencies generating maximum power for the three ILs are different. Considering viscosity $\eta_{[BMIm][N(CN)_2]} (27 \text{ cP}) < \eta_{[EMIm][BF_4]} (45 \text{ cP}) < \eta_{[BMIm][NO_3]} (168 \text{ cP})$, the optimal frequencies are $f_{\text{opt}[BMIm][N(CN)_2]} (28 \text{ Hz}) > f_{\text{opt}[EMIm][BF_4]} (22 \text{ Hz}) > f_{\text{opt}[BMIm][NO_3]} (12 \text{ Hz})$. For ILs with relatively small viscosity - [EMIm][N(CN)₂] and [EMIm][SCN], the effective power always increases with frequency in the range of 6-30 Hz. This means that the optimal frequencies of the two ILs are 30 Hz. It is interesting to note that the effective power $P_{[EMIm][BF_4]} > P_{[EMIm][SCN]}$ for frequencies smaller than 20 Hz, monotonously while that of [EMIm][BF₄] starts to decrease

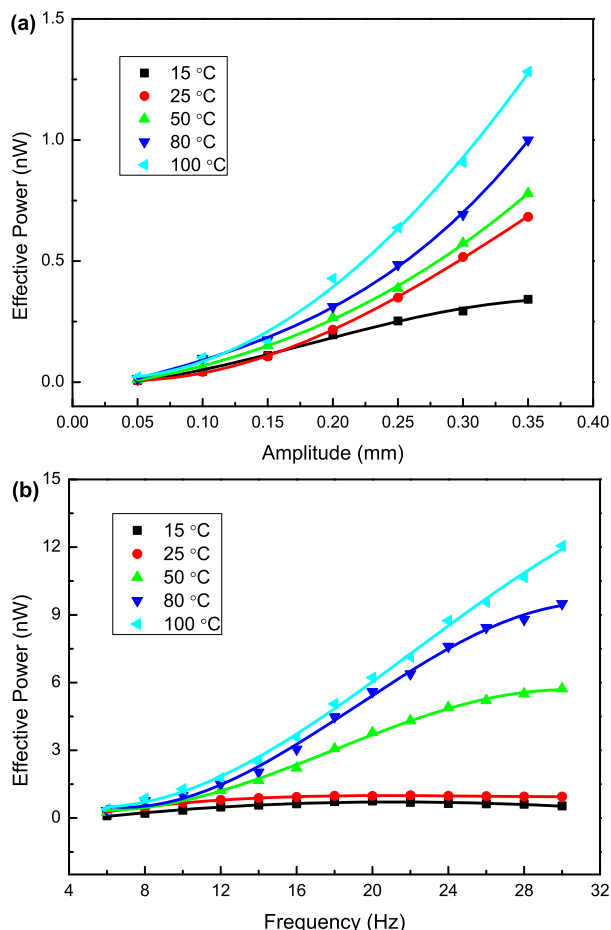


Fig. 5 (a) The effective power versus vibration amplitude L for different temperatures to [EMIm][BF₄] bridge with $f=10$ Hz and $R_L=30$ M Ω . (b) The effective power versus vibration frequency f for different temperatures to [EMIm][BF₄] bridge with $L=0.35$ mm and $R_L=30$ M Ω . Volumes of bridges are 15 μ L. Dots represent the actual experimental data while solid lines are the fitted results.

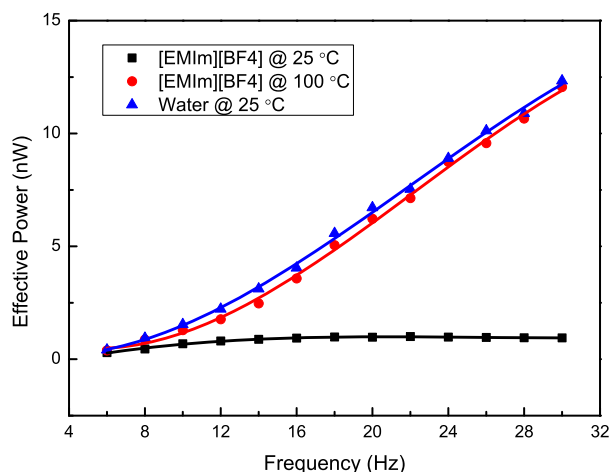


Fig. 6 The comparison of power generation of [EMIm][BF₄] bridge and water bridge with volumes of 15 μ L. Here, $L=0.35$ mm, $f=10$ Hz and $R_L=30$ M Ω . Dots represent the actual experimental data while solid lines are the fitted results.

in high frequency range. For the 15 μ L IL bridges, the generated maximum effective powers are about 2.1 nW for [EMIm][N(CN)₂], 1.7 nW for [BMIm][N(CN)₂], 1.2 nW for

[EMIm][SCN], 1.0 nW for [EMIm][BF₄] and 0.3 nW for [BMIm][NO₃] at their optimal vibration frequencies. To sum up, the imidazolium ILs with short alkyl chain and low viscosity can output more power in energy harvesting. The output powers are in the same orders of magnitude for several nanowatts with recent droplet based mechanical energy harvester^{16, 17}.

Water based VEH was only able to operate within narrow temperature range (0 to 60 °C) because of properties of water. However, ILs based VEH will probably work well even in 100 °C because of wide liquid temperature range and good thermal stability of ILs. So the performance of ILs based VEH at high temperature was further investigated. Because the better thermostability of [EMIm][BF₄], take [EMIm][BF₄] based VEH for example. Fig. 5 shows the effective power increases with increasing the temperature in the same vibration amplitude and frequency. This probably results from the decreased ion association in ILs with increasing temperature^{18, 19} and temperature-induced obvious decrease of viscosity^{20, 21}. An increase in the concentration of simple ions as a consequence of breakdown of aggregates results in adsorption more cations to top interface^{13, 22} and then the charge density near top interface increases, which improves the output power rapidly. Low viscosity guarantees large variation of the contact area between the ILs bridge and top plate during the vibration cycle. Large variation of the contact area leads to increase of power generation. As can be seen from Fig. 5(b), the optimal frequency shifts to the high frequency region when temperature increases. Especially at 100 °C, the effective power increases with vibration frequency monotonously and the maximum effective power can reach to 12.1 nW. Low viscosity at high temperatures reduces the viscosity induced damping on change of the top contact area and the combined effect with frequency increase is the monotonous improvement of the generated power at vibration frequency from 6 Hz to 30 Hz. Therefore, increasing temperature raises the power generation of the ILs based VEH.

Following, we compare the output effective power of [EMIm][BF₄] bridge and water bridge. The results are shown in Fig. 6. As one can see, the water based VEH can generate more power than [EMIm][BF₄] based VEH at 25 °C, especially at high vibration frequencies. The very small viscosity of water (about 1 cP) is responsible for this large difference. The power ratios of [EMIm][BF₄] to water are 0.70, 0.18 and 0.08 at 6 Hz, 18 Hz and 30 Hz, respectively. Because the viscosity plays the more important role in power generation at high frequencies, the difference of output power at high frequencies is larger. When operating temperature is 100 °C, the generated power of [EMIm][BF₄] based VEH improves substantially compared with that at 25 °C and approaches the water based VEH at 25 °C very much. This means that the output powers of ILs and water based VEHs⁸ are comparable.

To maximum the power output delivered to the load, the impedances of load and VEH should be matched and they should be minimized. The trend can be seen in Fig. 7. With increasing the load resistance, a local effective power maximum can be found at the optimal load resistance that

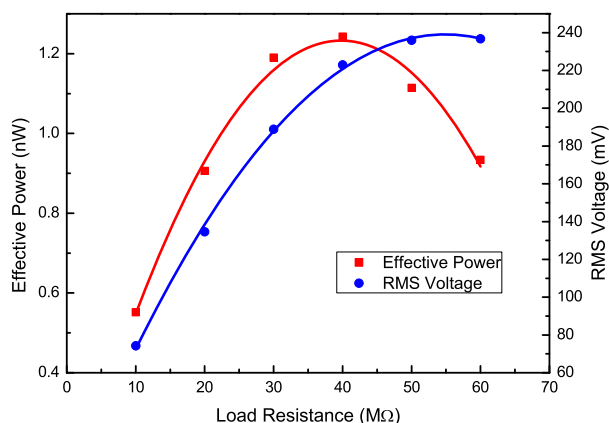


Fig. 7 The effective power and RMS voltage versus load resistance for 15 μL [EMIm][N(CN)₂] bridge with $L=0.35$ mm and $f=10$ Hz. Dots represent the actual experimental data while solid lines are the fitted results.

5 matches the source output impedance, while the RMS voltage increases monotonously. The [EMIm][N(CN)₂] based VEH can generate a maximum power of 1.24 nW for vibration at 10 Hz on an optimal load resistance of 40 M Ω . This experimental data is in good agreement with the electrical circuit model prediction of 38 M Ω .

In order to power for autonomous sensors, the effective power is needed to increase. One method is to form numerous small and equally sized IL bridges in parallel between two plates. It is estimated that ILs based VEH with 1 m² liquid-substrate overlap area (about 58000 IL bridges with considering bridge-bridge interspaces) will generate about 0.12 mW effective power at room temperatures and about 0.70 mW effective power at 100 °C. Another method is to use electret as dielectric film on the top plate. The electret is electrically charged dielectrics that can retain charges for years²³. Because electret can leads to the increase of the charge density near the interface between the ILs bridge and top plate, the effective power is expected to increase drastically.

25 In conclusion, the ILs based VEH by periodically squeezing liquid bridge has been proposed and demonstrated. The effects of physicochemical properties of ILs and operating temperature on power generation have been investigated. The results indicate that the VEH using imidazolium ILs with short alkyl chain and low viscosity can generate more power. Moreover, the output power of ILs based VEH improves with increasing the operating temperature and the output power at 100 °C reaches to about 22 times of that at 15 °C for [EMIm][BF₄]. Compared with water based EVH, the ILs based VEH need not be airtight sealed and can stably operate in the wide temperature range. Besides, the generated power of ILs based EVH affected by the physicochemical properties of ILs can be further improved through rational design and synthesis of ILs. At room temperatures, the maximum power density can reach to about 0.12 mW/m² while it is 0.70 mW/m² at 100 °C. We believe that this new energy harvester can be applied as a power source for self-sustainable wireless sensor networks and portable electronics with small power consumption in the near future.

Acknowledgements

This work was supported by the National Natural Science Foundation of China (No. 21373247 and No. 61205204), and the “Spring Sunshine” Plan (No. Z2011029).

Notes and references

^a School of Information Science and Engineering, Lanzhou University, Lanzhou 730000, China. E-mail: zxp@lzu.edu.cn

^b Centre for Green Chemistry and Catalysis, Lanzhou Institute of Chemical Physics, CAS, Lanzhou 730000, China. Fax: +86-931-4968116; Tel: +86-931-4968116; E-mail: ydeng@licp.cas.cn

† Electronic Supplementary Information (ESI) available: Details of the structure and characterization of ionic liquids, device fabrication and assembly, electrical circuit model, numerical calculations and other experimental result. See DOI: 10.1039/b000000x/

1. S. Roundy, E. S. Leland, J. Baker, E. Carleton, E. Reilly, E. Lai, B. Otis, J. M. Rabaey, P. K. Wright and V. Sundararajan, *IEEE Pervasive Comput.*, 2005, **4**, 28-36.
2. I. C. Lien and Y. C. Shu, *Smart Mater. Struct.*, 2012, **21**, 082001.
3. S. P. Beeby, R. N. Torah, M. J. Tudor, P. Glynn-Jones, T. O'Donnell, C. R. Saha and S. Roy, *J. Micromech. Microeng.*, 2007, **17**, 1257-1265.
4. Y. Naruse, N. Matsubara, K. Mabuchi, M. Izumi and S. Suzuki, *J. Micromech. Microeng.*, 2009, **19**, 094002.
5. D. Hoffmann, B. Folkmer and Y. Manoli, *J. Micromech. Microeng.*, 2009, **19**, 094001.
6. G. M. Whitesides, *Nature*, 2006, **442**, 368-373.
7. T. Krupenkin and J. A. Taylor, *Nat. Commun.*, 2011, **2**, 448.
8. J. K. Moon, J. Jeong, D. Lee and H. K. Pak, *Nat. Commun.*, 2013, **4**, 1487.
9. P. Sharma and T. S. Bhatti, *Energy Conv. Manag.*, 2010, **51**, 2901-2912.
10. A. Lewandowski and M. Galinski, *J. Phys. Chem. Solids*, 2004, **65**, 281-286.
11. M. Armand, F. Endres, D. R. MacFarlane, H. Ohno and B. Scrosati, *Nat. Mater.*, 2009, **8**, 621-629.
12. P. G. Degennes, *Rev. Mod. Phys.*, 1985, **57**, 827-863.
13. V. Lockett, R. Sedev, J. Ralston, M. Horne and T. Rodopoulos, *J. Phys. Chem. C*, 2008, **112**, 7486-7495.
14. X. Zhang, R. S. Padgett and O. A. Basaran, *J. Fluid Mech.*, 1996, **329**, 207-245.
15. D. J. Mollot, J. Tsamopoulos, T. Y. Chen and N. Ashgriz, *J. Fluid Mech.*, 1993, **255**, 411-435.
16. E. Yildirim and H. Kulah, *Microfluid. Nanofluid.*, 2012, **13**, 107-111.
17. Z. C. Yang, E. Halvorsen and T. Dong, *Appl. Phys. Lett.*, 2012, **100**, 213905.
18. R. Atkin and G. G. Warr, *J. Phys. Chem. C*, 2007, **111**, 5162-5168.
19. M. Mezger, H. Schroder, H. Reichert, S. Schramm, J. S. Okasinski, S. Schoder, V. Honkimaki, M. Deutsch, B. M. Ocko, J. Ralston, M. Rohwerder, M. Stratmann and H. Dosch, *Science*, 2008, **322**, 424-428.
20. J. Jacquemin, P. Husson, A. A. H. Padua and V. Majer, *Green Chem.*, 2006, **8**, 172-180.
21. X. D. Hu, S. G. Zhang, C. Qu, Q. H. Zhang, L. J. Lu, X. Y. Ma, X. P. Zhang and Y. Q. Deng, *Soft Matter*, 2011, **7**, 5941-5943.
22. M. Holovko, V. Kapko, D. Henderson and D. Boda, *Chem. Phys. Lett.*, 2001, **341**, 363-368.
23. S. Boisseau, G. Despesse and A. Sylvestre, *Smart Mater. Struct.*, 2010, **19**, 075015.

Graphical and Textual Abstract

Ionic liquids based vibration energy harvester can stably work in the wide temperature range (up to 100 °C) and generated power can be improved by rationally choosing ionic liquids.

